

Measurements of High Gradient Superconducting RF Cavities.

R.S. Orr

Department of Physics, University of Toronto, Canada

August 2006

As I described in my proposal to JSPS, I spent the term of my fellowship at KEK in Tsukuba working with a group whose research program is directed at the production of high gradient superconducting RF cavities. In this report I describe why the present state of high energy particle physics motivates physicists to envisage a new accelerator based on superconducting RF. I then describe the state of development of superconducting RF as of a year ago, and developments that I participated in during the term of my JSPS fellowship.

Particle Physics Today:

Five decades ago, there was very little understanding of the constituents of matter below the level of the nucleus. In addition the forces that governed the interaction of these constituents were mysterious. While a relativistic quantum field theory of electromagnetism existed, attempts to extend this to the so-called strong and weak nuclear forces were initially unsuccessful. In the decade from about 1965 to 1975 there were two break-throughs which led to our present apparently rather complete understanding of the structure of matter below the scale of the proton and the neutron.

The first break-through was theoretical in nature. It had long been understood that the weak nuclear force and the electromagnetic force were somehow intimately connected. In the late 1960s Salam, Ward, and Weinberg showed how these two forces could be understood as different aspects of a single electro-weak force. The theoretical mechanism used for this unification is known as “a spontaneously broken gauge symmetry”. This combined theory allows us to calculate electroweak processes to arbitrary accuracy. The theory made several profound and exciting predictions. Perhaps the most dramatic were the existence of new massive particles called the W and Z bosons, and the existence of a scalar particle produced in the spontaneous symmetry breaking process which gives mass to the W and Z . This scalar is known as the Higgs Boson. Within the standard model it is an elementary scalar particle. However, extensions to the standard model can incorporate several of these scalars, and there are models where the scalar particles are not elementary.

In the past 20 years, the standard model has been dramatically vindicated. At present all known sub nuclear phenomena can be incorporated within the standard model. The recent discovery of neutrino masses is extremely interesting, but these masses can be simply incorporated in the standard model without modifying any of its basic assumptions.

The one prediction of the standard model which has not been experimentally confirmed is the existence of an elementary scalar, such as the Higgs, or something which plays an analogous role in electroweak symmetry breaking. However, within the context of the standard model it is possible to use results from e^+e^- collisions at the CERN LEP collider, and $\bar{p}p$ collisions at the Fermilab Tevatron, to put stringent indirect limits on the mass of a standard model Higgs. The

most recent results are that the mass of the Higgs is limited by $m_H < 166 GeV$. If this result is true, then the Higgs will certainly be observed at the CERN Large Hadron Collider; probably round 2010.

The International Linear Collider:

The accepted opinion is that after the Higgs has been observed a high precision study of its coupling strengths will be required. These coupling strengths are predicted by the standard model, and a high precision study of them will confirm (or otherwise) that the particle observed at the LHC is indeed the Higgs. The past history of particle physics shows that e^+e^- colliders are the

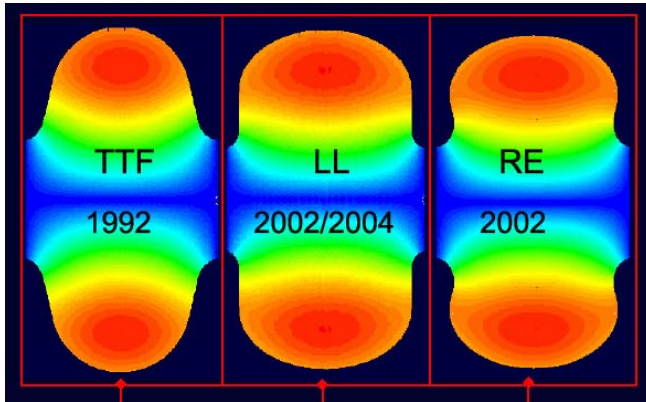


Figure 1 Shapes of various high gradient cavity designs.

	TESLA	LL	RE	IS
Diameter [mm]	70	60	66	61
E_0/E_{acc}	2.0	2.36	2.21	2.02
H_0/E_{acc} [Oe/MV/m]	42.6	36.1	37.6	35.6
R/Q [W]	113.8	133.7	126.8	138
G[W]	271	284	277	285
E_{acc} max	41.1	48.5	46.5	49.2

Table 1 Characteristics of new cavity designs.

best devices for making such a study. Much of the confirmation of the standard model was due to work at the LEP e^+e^- collider. LEP was a circular synchrotron storage ring machine, with a maximum centre of mass energy of $200 GeV$. A new e^+e^- collider designed to study the Higgs couplings would need a centre of mass energy of $500 GeV$. However, at this energy the synchrotron radiation from light electrons in a circular storage ring becomes a prohibitive source of energy loss. For this reason the particle physics community has proposed that the new machine be a linear collider. That is, beams of positrons and electrons will be accelerated in two long linear accelerators, and will collide head on at a central interaction point. While this machine design overcomes the problem of synchrotron radiation, it brings with it many technological challenges. In order to have a useful event rate, the colliding beams must be focused down to very much smaller cross sections than in existing machines. The required cross sections are $\sigma_x = 0.5 \mu m$ and $\sigma_y = 0.005 \mu m$. Since the overall length of the machine would be of order 30 km, these beam dimensions put a premium on the geometrical accuracy of the machine component alignment. The heart of a linear collider are the RF cavities, where the accelerating electric field is produced. Two years ago there were two possible approaches to building the ILC; a design based on room temperature X-band (10 GHz) cavities, and a superconducting design based on L-band (1.3GHz) cavities. Because of the high frequency necessary for the room temperature cavities, the alignment problems are particularly severe in this approach. At least partly for this reason, the International ILC Technology Recommendation Committee recommended in 2005 that the ILC should adopt the superconducting L-band cavities. This

decision was based on the existence of cavities produced at DESY (Tesla type cavities) which indicated with some reliability that maximum accelerating gradients of 35 MV/m could be attained, and that an operating gradient of 31 MV/m was feasible. The Tesla type cavities are probably are in the most developed state. However, recently, there have been developments which lead to the expectation that higher accelerating gradients are achievable. The Low Loss (LL) from JLAB/DESY, the Re-entrant (RE) and IS (KEK) cavity designs all show promise of reaching maximum gradients of 48 – 50 MV/m. This would allow the operating gradients of 36.0 MV/m and reduce the length (assuming 75% “fill factor”) of the ILC to of order 20 km. This reduction in the machine length would clearly lead to a large saving in the cost of the machine. A superconducting RF cavity goes normal when the critical magnetic field at the superconducting surface is exceeded. These new cavity designs aim to reduce the ratio of the peak magnetic field (H_p) to the accelerating field gradient (E_{acc}). Fig.1 shows the shape of the various recent designs, and Table1 shows the parameters of these designs.

The Author’s activities in the KEK High Gradient Cavity Group

When the author started his JSPS Fellowship at KEK, the High Gradient Superconducting RF group was just starting an extensive series of studies of the surface preparation of single cell cavities. While the cavities designed for the ILC are 9 cell structures, a rapid, high statistics study of the effect of cavity preparation on the achievable accelerating gradient is most easily done with single cell structures. The author took part in most aspects of the fabrication, surface preparation and testing of a series of six single cell cavities of the IS design. In terms of travel, I traveled to the company which produced the deep drawn cups for the cavity fabrication, Tokyo Denki which produced the Niobium blanks, and Nomura Plating which did the electropolishing. I also travel to the Toshiba Company in connection with the work on the high power coupler. The JSPS travel grant covered the cost of these trips.

I also participated in test of the RE, LL single cell cavities, and ICHIRO 9 cell designs. Finally, I worked on the assembly and testing of a high power RF coupler, designed to couple RF power into the ICHIRO 9-cell cavity.

During the tenure of the Fellowship, the author’s work resulted in three joint conference contributions.

1) EXPERIMENTAL COMPARISON AT KEK OF HIGH GRADIENT PERFORMANCE OF DIFFERENT SINGLE CELL SUPERCONDUCTING CAVITY DESIGNS, F. Furuta et al, Proceedings of European Conference of Particle Accelerators, Edinburgh, June 2006 .

2) SERIES TESTS OF HIGH-GRADIENT SINGLE-CELL SUPERCONDUCTING CAVITY FOR THE ESTABLISHMENT OF THE KEK RECIPE, T. Saeki et al, Proceedings of European Conference of Particle Accelerators, Edinburgh, June 2006 .

3) INITIAL STUDIES OF 9-CELL HIGH-GRADIENT SUPERCONDUCTING CAVITIES AT KEK, T. Saeki et al, Proceedings of LINAC2006, Oakridge, August 2006.

Fabrication of Single Cell Cavities.



Pure Niobium is the material of choice for the production of superconducting RF cavities. It has a relatively high transition temperature of 9.5 K, a relatively high critical magnetic field of 1980 gauss at 0 K, good thermal conductivity, and metallurgical properties close to those of copper.

Figure 2: Trimmed, deep drawn, pure niobium half cups.



Figure 3: Assembled single cell cavity structure.

The fabrication process started with the production at Tokyo Denki of circular blanks of pure niobium.

These circular blanks were then deep drawn in a high pressure press at a local company which specializes in pressing metal forms. The resulting half cups of the resonating structure are trimmed ready for electron beam welding into a complete single cell. The trimmed half cups can be seen in Fig.2.

The two half cups are first electron beam welded around the equator, to form the cavity itself. The niobium “beam pipes” are welded onto the “beam ports” on the cavity. Finally flanges are welded onto the ends of the beam pipes. These flanges allow the vacuum and RF power end pieces to be mounted on the cavity assembly

Surface Preparation of single cell cavities.

The first step in the surface preparation is to produce a mechanically smooth internal surface. While the surface of the blanks are quite smooth, the process of deep drawing, and electron beam welding, especially around the equator of the cavity itself, leaves a number of mechanical imperfections.

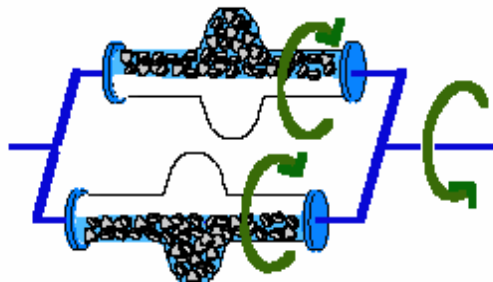


Figure 4: Schematic of the centrifugal barrel polishing process.

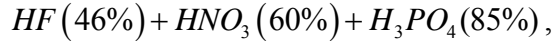
The process of centrifugal barrel polishing is designed to remove these mechanical imperfections by a process of mechanical abrasion. The process is shown schematically in Fig. 4. The cavity is filled with water and mechanical abrasive stones. The assembly is then mounted in a polishing machine which rotates the cavity at about 100 rpm, in the fashion shown in

Fig. 4. The cavity undergoes several passes through this process with successively finer abrasive. The total process may take as long as 30 hours of polishing, and the total amount of material removed from the surface is usually between 100 and 235 microns.



Figure 5: Light Chemical Polishing.

After the barrel polishing is complete, the contamination from the abrasive liquid must be removed from the cavity surface. This is done by a process known as Light Chemical Polishing (CP). The cavity is filled, by hand, with an acid solution, see Fig. 5. The acid solution is,



in equal proportions by volume. This treatment is done for 1 minute at $25^\circ C$ and removes about 10 microns from the internal surface.

After the CP the cavity is then annealed and degassed in a furnace at $750^\circ C$. During the CP process, a hydrogen rich layer forms on the surface of the cavity. The annealing process causes this hydrogen to diffuse deeply into the surface. This avoids a problem with the Q value of the cavity falling off at high accelerating gradient levels.

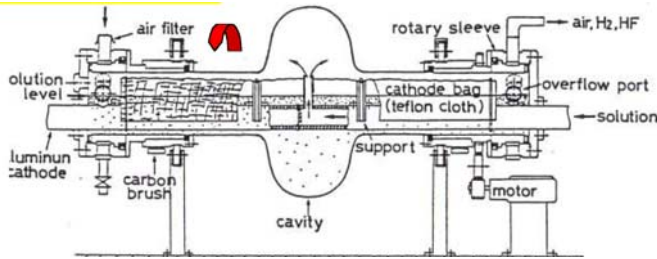
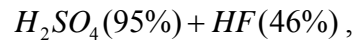


Figure 6: Electropolishing process

The final step in the surface preparation is known as Electro-Polishing. While in the past this has been carried out at KEK, for the cavities in this study, the EP of both the single cell and 9-cell cavities was performed by Nomura plating. The apparatus for the EP process is shown schematically in Fig. 6. A

photograph of the apparatus is shown in Fig. 7. The cavity is rotated slowly while filled with an acid solution. The usual composition of this acid is,



with a volume ratio of 10:1.



Figure 7: Electropolishing apparatus

inner surface of the cavity. The electropolishing process produces a very smooth surface, which can support high accelerating gradients.

Inside the cavity there is an aluminium cathode, and a current of about 40 A at 20 V is passed through a circuit which includes the cavity as an anode. The cathode is surrounded by a Teflon bag which prevents hydrogen gas bubbles from marking the



Figure 8: High pressure rinse

The electropolishing process may leave deposits on the inner surface of the cavity. The deposits may be products of the chemical reaction such as sulfur, or dust, or other particulate matter. In order to reach the very highest gradients, the cavities are cleaned in a high pressure water rinse. This process is shown in Fig.8. A nozzle projects into the cavity interior and sprays ultra pure water at 7 MPa, corresponding to a flow rate of 10 Liters/minute. During the rinsing process an automatic mechanism both rotates and lowers and raises the position of the cavity. This ensure that the complete surface of the cavity is subjected to the high pressure water spray. Normally cavities are subjected to this rinsing process for one hour.



Figure 9: Cavity assembled ready for cold testing.

The final accelerating gradient reached by a cavity depends quite strongly on the purity of the water used. The Nomura Plating Co. water used in most of these measurements had a specific resistance of $18\text{M}\Omega\text{cm}$, a total oxidisable carbon content of 12-22 ppb, and a bacteria content of 0 – 3 count/mL.

After the high pressure rinse the cavity is assembled for testing. The bottom flange incorporates a antenna used to inject RF power into the cavity. The position of this antenna may be remotely controlled. The bottom flange also incorporates a vacuum valve, which allows the cavity to be evacuated on a test stand, isolated, and transferred to the test cryostat. The top flange incorporates a fixed antenna, which couples to the RF power transmitted by the cavity during cold testing.

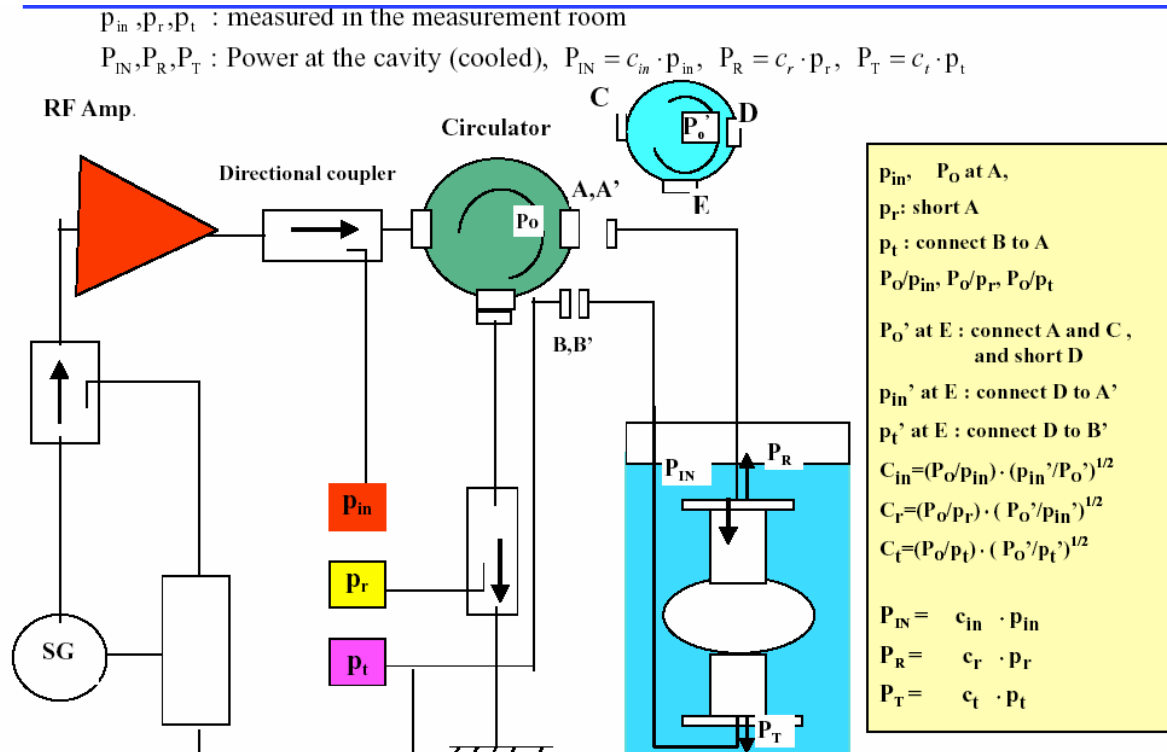


Figure 10. Schematic of the system used in making liquid helium temperature measurements of the accelerating gradients of single cell cavities.

Tests of Single Cell Cavities:

The principles behind Continuous Wave cold testing of the single cell cavities are shown in Fig: 10. The cavity is connected to the test system by two couplers, an input power antenna connected to an RF amplifier and a transmitted power coupler. During cold testing, the cavity is immersed in liquid helium in a cryostat at typically 2.0 K. The position of the input antenna can be remotely adjusted so that the reflected power is minimized. At each input power level, the input, reflected, and transmitted power are measured, allowing a calculation of the Q value of the cavity and the E_{acc} . The typical maximum E_{acc} are reached at input powers of around 50 Watts.

The power meters which measure the incident, reflected, and transmitted power levels are read out by a computer program, which then calculates the Q value of the cavity, and the accelerating gradient, E_{acc} . A measurement of a cavity consists of progressively increasing the input RF power to the cavity, and measuring the Q value and E_{acc} . Several phenomena can occur during the measurement of this excitation curve. The most noticeable phenomena are multi-pacting, and field emission of electrons. Both of these phenomena result from contaminants on the RF surface of the cavity lowering the work function for the emission of electrons from the surface. Multipacting is a resonant phenomenon at a particular gradient. The resonant gradient can often be exceeded by training the cavity, a process during which the contaminants are presumably "evaporated" from the cavity surface. Sometimes the contaminant cannot be removed by training, and multipacting may be a limitation on the gradient. The limitation comes from the fact that the energy deposited on the superconducting surface, by the multipacting electrons, may cause it to go normal, or "quench". When the cavity quenches, the Q value will drop by many orders of

magnitude, and the cavity will not be able to support high gradients. The second phenomenon is field emission. This is the non-resonant emission of electrons from the surface of the cavity. It has been established by many studies that field emission is caused by contaminants on the RF surface of the cavity, which act as field emitting centres. The field emission electrons are accelerated in the electric field in the cavity. Again, where they impact inside the cavity, they deposit energy, which may be enough to cause the cavity to quench.

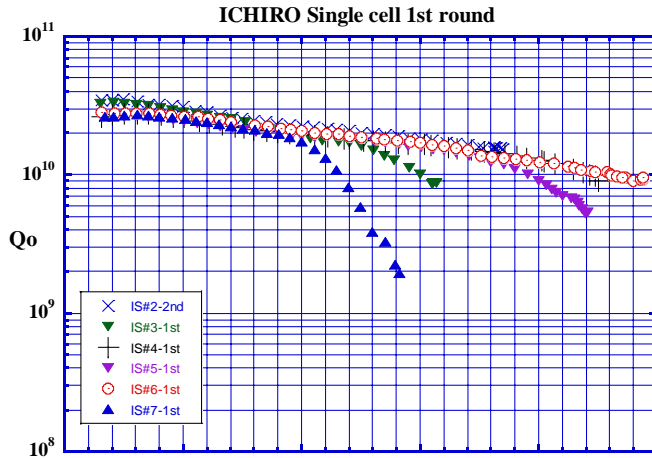


Figure 11 Typical excitation curves for single cell cavity measurements.

typical of field emission. As the gradient increases, more and more electrons are emitted, and this electron cloud starts to absorb all the available RF power, leading to the drop of the Q value. That this happens at different rates, is due to the distribution of the size of the contaminating field emission centres. The field emission centres can originate from almost anywhere in the cavity

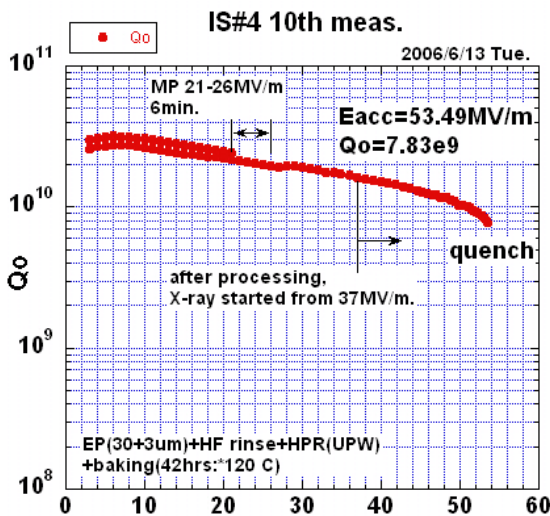


Figure 12: Detailed excitation curve for a cavity which achieved close to the theoretical

A typical set of measurements on four different cavities is shown in Fig. 11. All of these cavities were prepared in the same fashion. However, it is clear that they go to very different maximum gradients. The red (circular) points correspond to a cavity which essentially reaches the maximum theoretical accelerating gradient. In this cavity quenching occurs when the surface magnetic field at some point in the cavity exceeds the critical value. The three sets of triangular points show the Q value of the cavity dropping off rapidly as the accelerating gradient increases. This is

preparation process. However, it is most likely that they are from the ultra pure water, or are due to the level of contamination in the assembly clean room.

Fig.12 shows in detail the measurement of a typical cavity which achieved the theoretical maximum in accelerating gradient. As the input power was increased, there was an initial period of multipacting at around 20 MV/m. After the contaminant leading to the multipacting “evaporated”, it was possible to increase the accelerating gradient up to the theoretical maximum. The X-rays are due to field emission electrons which bremsstrahlung when they hit the cavity walls. These X-rays indicate that the cavity still had some residual surface contamination. This probably led to the drop of in Q-value at high gradient.

A Statistical Study of the Single Cell Cavity Measurements.

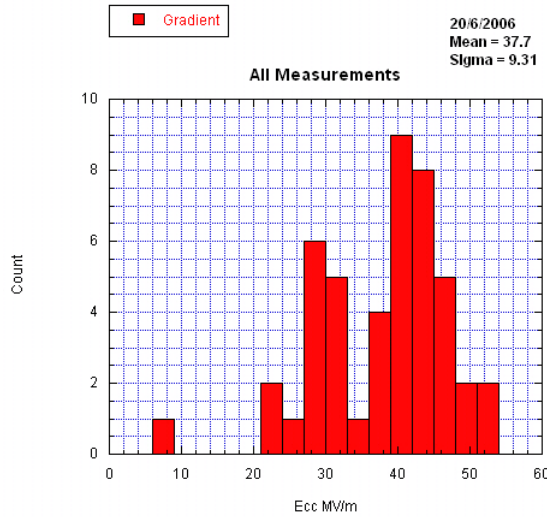


Figure 13: Overall distribution of maximum accelerating gradient for all cavities measured.

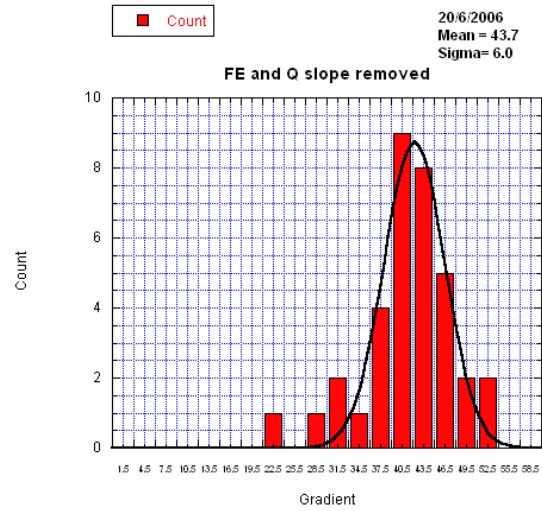


Figure 14: Distribution of maximum measured gradients, when field emission and Q-slope

The author performed a statistical study of this series of measurements on the single cell cavities. The various phenomena occurring in the cavities are all presumably stochastic in nature, and an overall understanding can best be attained by studying the measurements as a statistical population. Fig. 13 is the distribution of all measurements of the accelerating gradients of the single cell IS cavities. Repeated measurements of the same cavity are included in this plot. One

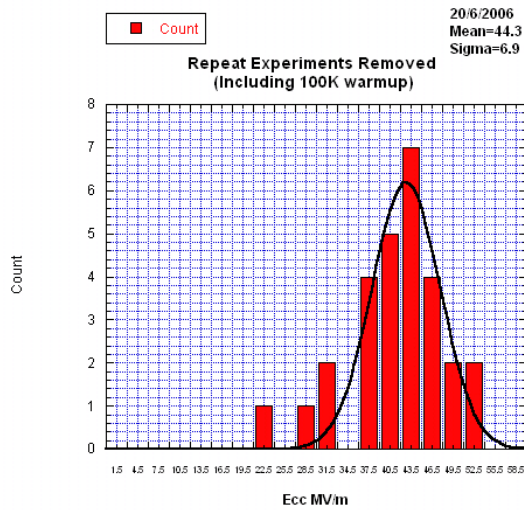


Figure 15: Distribution of maximum measured accelerating gradient when double

sees three regions. There is one cavity at a very small maximum gradient of less than 10 MV/m. This corresponds to a cavity that was probably grossly contaminated, and has a very severe level of field emission. There is a population of a few cavities at maximum gradients of around 20 MV/m. These are cavities where the level of contamination is such that the multipacting barrier cannot be over come. There is a very distinct population centred at 30 MV/m. These are cavities where the level of non-resonant field emission limits the maximum gradient. The sharp peak may well be indicative of the size of the contaminating field emitters. With more work, it would be possible to perhaps localize the source of these emitters. In Fig. 14, all measurements where there was strong field emission, or rapid Q drop off (probably due to hydride formation), have been

omitted. This population represents cavities which have a low residual level of contamination, and likely reach the theoretical maximum. The spread is due to the local characteristics of the cavities, measurement uncertainties, and perhaps a low level of very small field emitters. Fig 14 contains some double counting. Some cavities were measured several times without being warmed above 100 K. This double counting is removed in Fig. 15.

The population in Fig. 15 shows the distribution of accelerating gradients achievable by the IS shape when there is essentially no residual contamination resulting in field emission limitation of the maximum accelerating gradient. The population is well represented by a Gaussian distribution $44.3 \pm 6.9 \text{ MV} / \text{m}$.

Conclusion.

These measurements of single cell cavities indicate that surface preparation methods are known which could, in principle, be used to produce ILC 9-cell cavities with a working gradient of 36 MV/m . At the time of writing, these high gradients have not been achieved with 9-cell cavities. One simple hypothesis is that in an environment (high pressure rinse, clean room, etc) with a given level of contamination, the probability of contamination is roughly proportional to the internal surface area of the cavity. If this is true, then high gradients will be achieved in 9-cell cavities through careful optimization of water purity, clean room level, and the procedures used for the assembly of the cavities.